



Age-related changes in the proteostasis network in the brain of the naked mole-rat: Implications promoting healthy longevity



Judy C. Triplett^a, Antonella Tramutola^b, Aaron Swomley^a, Jessime Kirk^a, Kelly Grimes^{c,d}, Kaitilyn Lewis^{c,e}, Miranda Orr^{c,d}, Karl Rodriguez^{c,d}, Jian Cai^f, Jon B. Klein^f, Marzia Perluigi^b, Rochelle Buffenstein^{c,d}, D. Allan Butterfield^{a,g,*}

^a Department of Chemistry, University of Kentucky, Lexington, KY 40506, United States

^b Department of Biochemical Sciences, Sapienza University of Rome, Piazzale Aldo Moro 5, 00185 Rome, Italy

^c Sam and Ann Barshop Institute for Longevity and Aging Studies, University of Texas Health Science Center, San Antonio, TX 78245, United States

^d Department of Physiology, University of Texas Health Science Center, San Antonio, TX 78245, United States

^e Department of Cellular and Structural Biology, University of Texas Health Science Center, San Antonio, TX 78245, United States

^f Department of Nephrology and Proteomics Center, University of Louisville, Louisville, KY 40202, United States

^g Sanders-Brown Center on Aging, University of Kentucky, Lexington, KY 40506, United States

ARTICLE INFO

Article history:

Received 27 April 2015

Received in revised form 13 July 2015

Accepted 1 August 2015

Available online 4 August 2015

Keywords:

Naked mole-rat

Proteomics

Phosphoproteomics

Aging

Proteostasis networks

mTOR

ABSTRACT

The naked mole-rat (NMR) is the longest-lived rodent and possesses several exceptional traits: marked cancer resistance, negligible senescence, prolonged genomic integrity, pronounced proteostasis, and a sustained health span. The underlying molecular mechanisms that contribute to these extraordinary attributes are currently under investigation to gain insights that may conceivably promote and extend human health span and lifespan. The ubiquitin–proteasome and autophagy–lysosomal systems play a vital role in eliminating cellular detritus to maintain proteostasis and have been previously shown to be more robust in NMRs when compared with shorter-lived rodents. Using a 2-D PAGE proteomics approach, differential expression and phosphorylation levels of proteins involved in proteostasis networks were evaluated in the brains of NMRs in an age-dependent manner. We identified 9 proteins with significantly altered levels and/or phosphorylation states that have key roles involved in proteostasis networks. To further investigate the possible role that autophagy may play in maintaining cellular proteostasis, we examined aspects of the PI3K/Akt/mammalian target of rapamycin (mTOR) axis as well as levels of Beclin-1, LC3-I, and LC3-II in the brain of the NMR as a function of age. Together, these results show that NMRs maintain high levels of autophagy throughout the majority of their lifespan and may contribute to the extraordinary health span of these rodents. The potential of augmenting human health span via activating the proteostasis network will require further studies.

© 2015 Elsevier B.V. All rights reserved.

1. Introduction

The bathyergid rodent, *Heterocephalus glaber*, more commonly known as the naked mole-rat (NMR) or sand puppy, is a strictly

subterranean rodent indigenous to North East Africa. Phylogenetically, these rodents are closely related to the guinea pig (*Cavia porcellus*); although comparative studies with NMRs often include other closely related rodents such as mice and rats [1,2]. NMRs are arguably best known because of their unusually long, healthy life spans (15–30 years) when compared with those of the traditional rodent models including mice and rats (1–3 years) [3–6]. This prolonged health span has led to research involving many cellular systems thought to contribute to the aging process including: oxidative stress or damage of biomolecules (i.e., proteins and nucleotides), mitochondrial dysfunction, and the autophagy/proteostasis network [7–11]. The ability of the NMR to withstand the chronic insult of protein unfolding stressors has been attributed to the efficiency with which the rodent maintains the integrity of its proteome by way of a high functioning proteostasis network [12–16]. The proteostasis network is a network of mechanisms in

Abbreviations: NMR, naked mole-rat; mTOR, mammalian target of rapamycin; LC3, microtubule-associate protein 1A/1B-light chain 3; UPS, ubiquitin–proteasome system; PGPH, post-glutamyl peptide-hydrolyzing; ChT-L, chymotrypsin-like; HSP, heat shock protein; ALP, autophagy–lysosomal pathway; IEF, isoelectric focusing; DDT, dithiothreitol; AI, iodoacetamide; ACN, acetonitrile; VDAC, voltage-dependent anion channel; Ub, ubiquitin; UBE1, Ub-like modifier-activating enzyme 1; UBE2, Ub-conjugating enzyme E2; UCH, Ub-carboxy terminal hydrolase; PSβ1, proteasome subunit beta type 1.

* Corresponding author at: Department of Chemistry and Sanders-Brown Center on Aging, University of Kentucky, Lexington, KY 40506-0055, United States.

E-mail addresses: Buffenstein@UTHSCSA.edu (R. Buffenstein), dabcns@uky.edu (D.A. Butterfield).

place to prevent and eliminate protein misfolding, and promotes degradation of unwanted and damaged organelles and proteins. This network contains the ubiquitin–proteasome system (UPS) and cellular autophagy, among others.

The UPS functions to maintain cellular proteostasis by degrading unwanted, misfolded or damaged proteins that could otherwise aggregate into potentially cytotoxic moieties, and UPS dysfunction has been implicated in multiple neurodegenerative disorders [17–21]. The proteasome cleaves damaged proteins into smaller peptide fragments by the proteolytic center that contains trypsin-like (T-L), post-glutamyl peptide-hydrolyzing (PGPH), and chymotrypsin-like (ChT-L) specificities [22,23]. Liver and brain samples from NMRs when compared with mouse controls, have shown increased ChT-L and T-L activities, suggesting a more efficient UPS that may contribute to their inherent resistance to aging and age-related diseases [8,14]. Moreover, human, mouse, and yeast proteasomes were demonstrated to have an increased activity when exposed to proteasome depleted cytosolic fractions containing a novel heat shock protein (HSP)-containing complex from NMR samples [23].

The autophagy–lysosomal pathway (ALP) is an evolutionarily conserved catabolic process by which the cell removes and recycles complexes, protein aggregates and damaged organelles [24]. Often observed as a mechanism to address starvation and reduce energy output, autophagy can also contribute to cellular differentiation, growth control, defense from xenobiotics, as well as general house-keeping and maintenance [25]. Thus, autophagy is generally thought of as a survival mechanism. ALP involves a number of proteins such as Beclin-1 and LC3 that are crucial in the initiation and recruitment of the autophagosome, which once formed, engulfs the target prior to fusing with the lysosome for recycling [26]. Further, the PI3K/Akt/mTOR axis plays a central role in cellular proteostasis as mTOR activation inhibits autophagy, and mTOR is a direct target of the kinase Akt, which is regulated by PI3K. Dysregulation of these pathways has been linked to neurodegenerative diseases [27–33].

A failing proteostasis network in the brain in particular increases vulnerability to dysfunctions in UPS and ALP due to the unique shape of neurons and their non-mitotic nature [34]. Further, these protein degradation mechanisms are essential in neuron function including neurotransmission and synaptic remodeling [35,36]. Dysregulation of these proteostasis maintenance systems can lead to neurodegeneration, diminished quality of life and reduced lifespan [37].

In the current age-related study of the NMR proteome and phosphoproteome, a large number of significantly altered brain proteins were identified, whose functions were related to metabolism, proteostasis networks, cellular signaling, structure, and neuronal plasticity. Too many proteins were identified to be efficiently discussed and expounded upon in a single manuscript; consequently, we facilitated discussion of the results by means of protein functionality. Here, we report on significant changes in proteins related to proteostasis and autophagy systems in the NMR brain and their impact upon the unusually long and salubrious lifespan of the NMR.

2. Materials and methods

2.1. Materials

Criterion precast polyacrylamide gels, TGS and MOPS electrophoresis running buffers, ReadyStrip IPG strips, mineral oil, Precision Plus Protein All Blue Standards, Sypro Ruby protein stain, biolytes, urea, dithiothreitol (DTT), iodoacetamide (IA), and nitrocellulose membranes were purchased from Bio-Rad (Hercules, CA, USA). Pro-Q Diamond phosphoprotein stain, anti-phosphotyrosine, anti-phosphoserine, and anti-phosphothreonine antibodies were procured from Invitrogen (Grand Island, NY, USA). Protein A/G beads Amersham ECL IgG horseradish peroxidase-linked secondary antibodies, and ECL Plus Western blotting detection reagents were purchased from GE Healthcare

(Pittsburgh, PA, USA). C₁₈ ZipTips and ReBlot Plus Strong stripping solution were obtained from Millipore (Billerica, MA, USA). Modified trypsin solution was purchased from Promega (Madison, WI, USA). Pierce BCA protein assay reagents A and B were purchased from Thermo Scientific (Waltham, MA, USA). Anti-p-PI3K (Tyr⁵⁰⁸) (sc-12929) and anti-BAP1 (Ub carboxyl-terminal hydrolase) (sc-28236) antibodies were purchased from Santa Cruz Biotechnology (Dallas, TX, USA). Anti-Beclin-1 (3738), anti-p-mTOR (Ser²⁴⁴⁸) (5536-S), anti-mTOR (2983-S), anti-AKT (4685-S), and anti-p-AKT (Ser⁴⁷³) (4058-S) antibodies were obtained from Cell Signaling Technology (Danvers, MA, USA). Anti-LC3-I and anti-LC3-II antibodies (NB100-2220) were purchased from Novus (Littleton, CO, USA). Anti-VDAC2 antibody (ab118872) was purchased from Abcam (Cambridge, MA, USA). All other chemicals used in this study were purchased from Sigma-Aldrich (St. Louis, MO, USA).

2.2. Animals

Brains from NMRs were obtained from well-characterized colonies [3] maintained by Dr. Rochelle Buffenstein at the University of Texas Health Science Center, San Antonio. The NMRs were housed in fabricated burrow systems under climate conditions that mimicked their natural habitat (30 °C and 30–50% relative humidity). The NMRs were fed ad libitum a diet that consisted of fresh fruits and vegetables, which was supplemented with a high protein and vitamin enriched feed (Pronutro, South Africa). NMRs were anesthetized with isoflurane, euthanized by cardiac exsanguination and the brains were immediately harvested and flash frozen in liquid nitrogen. All animal procedures were approved by the Institutional Animal Care and Use Committee at the University of Texas Health Science Center at San Antonio, TX. Experimental animal groups consisted of 5–9 individual brains from both male and female individuals and of both subordinate and breeding status. NMRs were divided into four age groups for analysis: 2–3 year-olds (age group 1; young; n = 6; 3 males/3 females), 4–6 year-olds (age group 2; intermediate; n = 7; 3 males/4 females), 7–12 year-olds (age group 3; old; n = 7; 4 males/3 females) and 15–24 year-olds (age group 4; oldest; n = 9; 4 males/5 females).

2.3. Sample preparation

Naked mole-rat whole brain homogenates were prepared using a Wheaton glass homogenizer (~40 passes) and diluted with ice-cold isolation buffer [0.32 M sucrose, 2 mM EDTA, 2 mM EGTA, 20 mM HEPES, 0.2 µg/mL PMSF, 5 µg/mL aprotinin, 4 µg/mL leupeptin, 4 µg/mL pepstatin, and 10 µg/mL phosphatase inhibitor cocktail 2]. Homogenate protein concentrations were ascertained by the Pierce BCA method (Rockford, IL, USA) [38].

2.4. Two-dimensional polyacrylamide gel electrophoresis (2-D PAGE)

2.4.1. Isoelectric focusing (IEF)

2-D PAGE experiments were performed as previously described [39]. In brief, 200 µg of each homogenate, suspended in 200 µL of rehydration buffer [8 M urea, 2 M thiourea, 50 mM DTT, 2.0% (w/v) CHAPS, 0.2% Biolytes, 0.01% bromophenol Blue], was sonicated and applied to 11 cm pH 3–10 ReadyStrip IPG strips. The strips were actively rehydrated and isoelectrically focused. At the end of the run, IPG strips were immediately stored at –80 °C.

2.4.2. SDS PAGE

IEF strips were thawed and equilibrated in DTT and IA-containing buffers. IEF strips were rinsed in a TGS running buffer before placement into 11 cm Criterion precast linear gradient polyacrylamide gels (8–16% Tris–HCl). Precision Plus Protein All Blue molecular standards and samples were run at a constant voltage of 200 V for approximately 65 min at 22 °C in Tris/Glycine/SDS running buffer.

2.5. Sypro Ruby and Pro-Q Diamond staining

After 2-D-PAGE, gel staining was carried out according to manufacturer's directions and as described previously [40]. Briefly, gels were incubated in 50 mL of fixing solution [10% (v/v) acetic acid, 50% (v/v) methanol], washed in deionized (DI) water, and stained with 60 mL of Pro-Q Diamond for 90 min. Gels were then destained four times in 100 mL of solution [20% acetonitrile (ACN), 50 mM sodium acetate, pH 4] for 30 min each. The gels were washed three times in DI water (30 min each) and then scanned at 580 nm using a Bio-Rad ChemiDoc XRS + imaging system (Bio-Rad, Hercules, CA, USA). Next, 50 mL of Sypro Ruby protein gel stain was added and allowed to incubate overnight (15 h). Gels were then rinsed in DI water, scanned at 450 nm with the ChemiDoc imager, and stored in DI water at 4 °C until protein spot extraction.

2.6. Image analysis

2.6.1. Expression proteomics

Spot intensities from SYPRO Ruby-stained 2-D-gel images of NMR brain samples were quantified according to the total spot density using PDQuest 2-D Analysis Software (Bio-Rad, Hercules, CA, USA). Intensities of individual spots were normalized to the total gel densities. Normalized spot densities of the four age groups (2–3 year-olds, 4–6 year-olds, 7–12 year-olds, and 15–24 year-olds) were compared. Only spots with statistically significant differences ($p < 0.05$) were considered for in-gel trypsin digestion and protein identification by MS/MS.

2.6.2. Phosphoproteomics

Protein spots from Pro-Q Diamond-stained 2-D-gel images of the NMR brain samples were quantified and matched as described

previously [40]. Next, a high match analysis between the master gels from the Sypro Ruby matching and Pro-Q Diamond matching was conducted. The phosphoprotein spot densities were normalized to the Sypro Ruby spot densities and the resultant normalized spot densities in four age groups were compared and spots that were statistically significant ($p < 0.05$) were considered for in-gel trypsin digestion and protein identification by MS/MS.

2.7. In-gel trypsin digestion/peptide extraction

Protein spots identify as significantly altered from the earliest age group were excised from 2-D-gels and transferred to individual Eppendorf microcentrifuge tubes for trypsin digestion as described previously [41]. In brief, DTT and IA were used to break and cap disulfide bonds and the gel plug was incubated overnight at 37 °C with shaking in a modified trypsin solution. Salts and contaminants were removed from the tryptic peptide solutions using C₁₈ ZipTips. Tryptic peptide solutions were reconstituted in 10 μ L of a 5% ACN/0.1% formic acid (FA) solution and stored at –80 °C until MS/MS analysis.

2.8. NanoLC–MS with data dependent scan

Tryptic peptide solutions were analyzed by a nanoAcquity (Waters, Milford, MA)-LTQ Orbitrap XL (Thermo Scientific, San Jose, CA) platform with a data dependent scan mode. An in-house packed capillary column (0.1 \times 130 mm column packed with 3.6 μ m, 200 Å XB-C18) was used for separation with a gradient using 0.1% FA and ACN/0.1% FA at 200 nL/min. The spectra obtained by MS were measured by the orbitrap at 30,000 resolution; and the MS/MS spectra of the six most intense parent ions in the MS scan were acquired by the orbitrap at 7500 resolution. The latest version

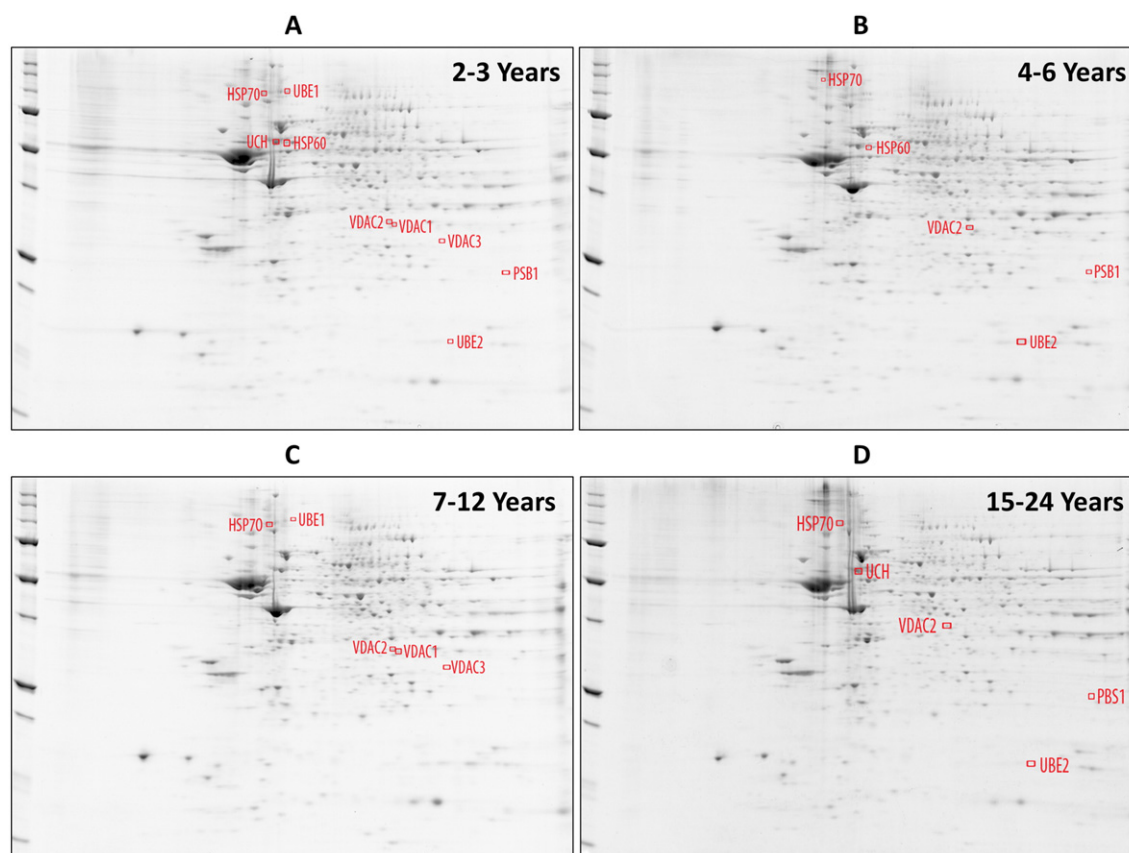


Fig. 1. Representative Sypro Ruby-stained 2-D gel images of isolated proteins from the brains of NMRs, aged 2–3 years (A), 4–6 years (B), 7–12 years (C), and 15–24 years (D). Proteins whose expression and/or phosphorylation state were significantly altered ($p < 0.05$) in the particular age group are labeled in the images.

of the Swiss-Prot database by SEQUEST (Proteome Discoverer v1.4, Thermo Scientific) was used to interrogate the data files of each sample. At least two high-confidence peptide matches were used for protein identification where the false discovery rate is <1%. Proteins that were matched with the same peptides were reported as one protein group. Protein data reported from these analyses include: the SwissProt accession number, the percentage of the protein sequence identified by matching peptides, the number of peptide sequences detected by the MS/MS analysis, the confidence score of the protein, and the expected molecular weight and predicted isoelectric point (pI).

2.9. Immunoprecipitation and Western blotting

2.9.1. Immunoprecipitation (IP)

Individual NMR brain homogenates (250 µg) were suspended in 500 µL of IP buffer [0.05% NP-40, aproprotin 5 µg/mL, leupeptin 4 µg/mL, pepstatin 4 µg/mL, and phosphatase inhibitor cocktail 10 µg/mL] in a phosphate buffer solution, pH 8 [8 M NaCl, 0.2 M KCl, 1.44 M Na₂HPO₄, and 0.24 M KH₂PO₄]. Samples were precleared by incubation with Protein A/G agarose beads for 1.5 h at 4 °C. Next, each sample was incubated overnight with anti-VDAC 2 antibody (1:50 dilution) at 4 °C. Samples were then incubated with Protein A/G agarose beads for 1.5 h at 4 °C and washed 5 times with IP buffer, preserving the beads for a 1D-PAGE experiment.

2.9.2. One-dimensional polyacrylamide gel electrophoresis (1-D-PAGE)

Sample homogenates (50 µg) or beads from VDAC2 immunoprecipitation experiment were suspended in 4× sample loading buffer [0.5 M Tris, pH 6.8, 40% glycerol, 8% SDS, 20% β-mercaptoethanol, 0.01% Bromophenol Blue] (diluted to 1× with DI water) and then heated at 95 °C for 5 min. Samples were cooled on ice and then loaded into Criterion precast 18 well polyacrylamide gels (4–12% Bis–Tris) or Criterion 12% TGX stain-free polyacrylamide 18 well gels. Using XT MOPS or TGS running buffer, gels were run at 80 V for 15 min and then at 120 V for approximately 100 min. Stain-free gels were scanned using a Bio-Rad ChemiDoc XRS+ imaging system to measure the total protein load before protein transfer to Western blots.

2.9.3. 1-D-Western blotting

In-gel proteins were transferred to a nitrocellulose membrane (0.2 nm) using a Trans-Blot Turbo Blotting System (Bio-Rad, Hercules, CA, USA) at 25 V for 30 min. After the transfer, membranes were incubated in a blocking solution (3% bovine serum albumin (BSA) in TBS-T [8 M NaCl, 2.4 M Tris, and 0.1% (v/v) Tween 20]) for 1.5 h. The membrane was then incubated with primary antibodies: VDAC2 and UCH (1:3000 dilution), tubulin (1:5000), and phosphoserine, phosphothreonine and phosphotyrosine antibodies (1:6000) and mTOR, p-mTOR (Ser²⁴⁴⁸), Akt, p-AKT (Ser⁴⁷³), p-PI3K (Tyr⁵⁰⁸) (1:1000 dilution), which were added to the blocking solution with gentle rocking for 2 h. The blots were washed three times with TBS-T (5 min each) and incubated with a horseradish peroxidase secondary antibody in TBS-T (1:5000) with gentle rocking. The membranes were then washed three more times in TBS-T (10 min each). Using a Clarity Western ECL substrate, membranes were chemiluminescently developed in the dark for 5 min, scanned using the ChemiDoc XRS+ imaging system, and quantified using Image Lab software (Bio-Rad, Hercules, CA, USA). Blots were stripped up to two times with ReBlot Plus Strong solution (15 min each) followed by three rinses with TBS-T (5 min each). Proteins were normalized either to total protein load of the gel or to tubulin. For the VDAC2 immunoprecipitation experiment, the phosphorylated amino acid residues in the VDAC2 protein were normalized to the total amount of VDAC2 protein in the Western blot.

2.10. Statistical analysis

A conservative analysis was carried out on PDQuest data using both a two-tailed Student's t-test and a Mann–Whitney U statistical test, independently comparing each age group to the youngest age cohort. Protein spots were considered statistically significant if $p < 0.05$ in both tests. To further determine significant differences ($p < 0.05$) between all of the various age groups, a one-way ANOVA with post hoc Bonferroni t-test was used. Protein spot fold-change values were calculated by dividing the average, normalized spot intensities of the gels of older age group by the average, normalized spot intensities of the gels of the younger age group in the comparison. For Western blot data, a one-way ANOVA with either a post hoc Bonferroni or Dunnett's multiple comparisons test was used. All data are presented as mean ± SEM. To ensure a rigorously conservative approach, spots were extracted for MS/MS analysis only if the fold change was 40% or greater or smaller in normalized spot density. Identifications of proteins acquired with the SEQUEST search algorithm were considered to be statistically significant if $p < 0.01$. At least two peptide sequences were used to identify each protein. To ensure a correct identification of the proteins, a visual comparison was made between the expected molecular weight and isoelectric point of the identified protein to the spot of the extracted 2-D gel plug.

3. Results

3.1. Age-related changes in proteins of the proteostasis network

Proteostasis network-related proteins with statistically significant changes with age in protein levels and phosphorylation states are labeled in the 2-D gel images of Figs. 1 & 2, respectively. PDQuest analyses of all 2-D gels found 9 proteostasis network-related proteins with significant changes in the NMR brain as a function of age (Table 1). Many of these proteins are associated with the UPS. Significant elevation of heat shock protein (HSP) response with age was noted by the increased levels of HSP70 protein 4 (Fig. 3A) and the decreased phosphorylation levels of HSP60 (Fig. 3B). While the primary function of HSP is to maintain a protein's native 3-D conformation, if a protein is terminally misfolded, some HSPs also function to chaperone the protein for UPS degradation. The UPS, illustrated in Fig. 4, depicts other significantly altered proteins with age of the NMR brain. Two of these proteins are involved in protein ubiquitylation: ub-like modifier-activating enzyme 1 (UBE1) and ub-conjugating enzyme E2 variant 2 (UBE2v2). Both exhibit decreased phosphorylation levels in the older age cohorts, further supporting the notion of increased UPS activity in the NMR with age is the increased expression of ub-carboxy-terminal hydrolase (UCH), the protein responsible for the removal of poly Ub chain, one Ub at a time from the C-terminal end, before entry into the proteasome. Interestingly, a component of the central proteasome itself, proteasome subunit beta type 1 (PSβ1), showed decreased phosphorylation levels in the intermediate and oldest age cohorts (Table 1).

Autophagy-related proteins with altered levels and/or phosphorylation states in one or more age cohorts include all three isoforms of the voltage-dependent anion channel (VDAC): VDAC1, VDAC2, and VDAC3. VDACS are the major outer mitochondrial membrane porins and regulators of energy metabolism and mitophagy. Levels of both VDAC2 and VDAC3 were significantly increased in the old age group as compared with control (Table 1), while phosphorylation levels decreased with age for all VDACS (Fig. 3C).

3.2. Immunoprecipitation and Western blotting validations

Immunoprecipitation and Western blot experiments were conducted on selected proteins to confirm MS/MS results. Western blot analysis of UCH (Fig. 5A) confirmed a significant increase in the level of UCH in

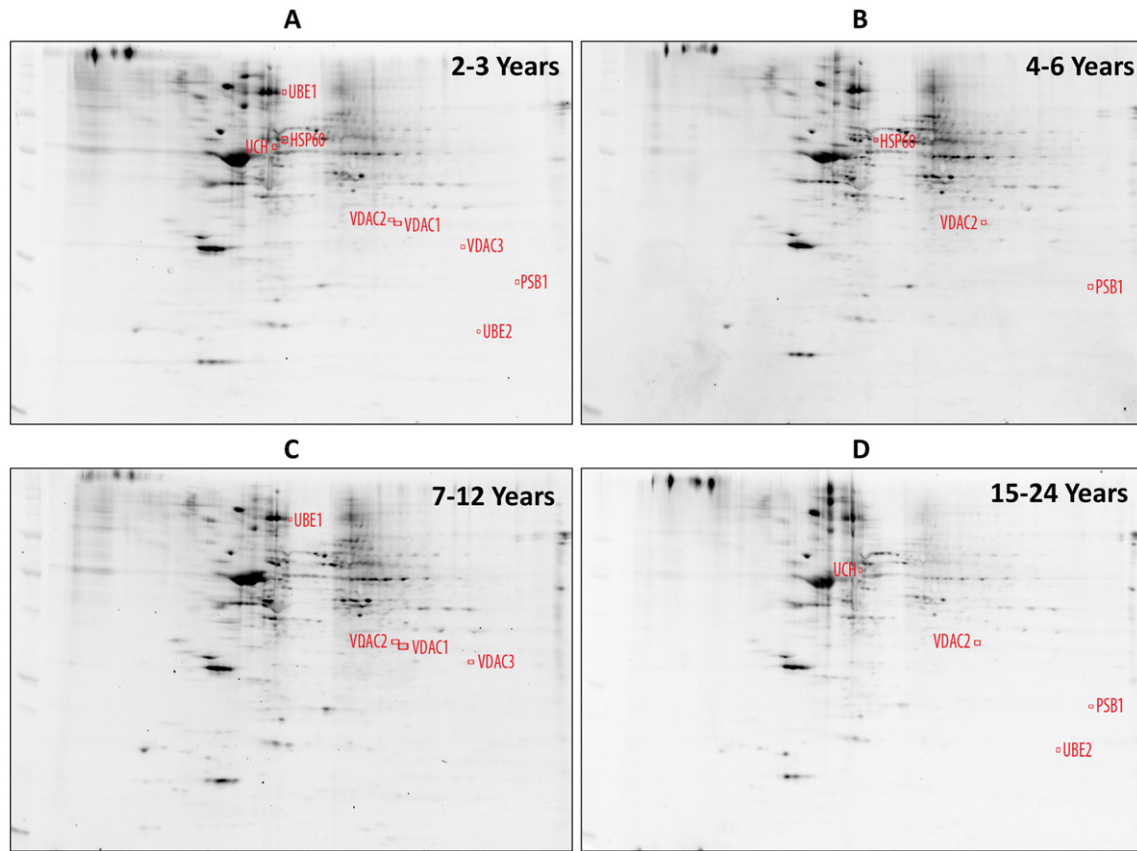


Fig. 2. Representative Pro-QDiamond-stained 2-D gel images of isolated proteins from the brains of NMRs, aged 2–3 years (A), 4–6 years (B), 7–12 years (C), and 15–24 years (D). Proteins with significantly altered phosphorylation levels ($p < 0.05$) in the particular age group are labeled in the images.

the brains of the oldest age group ($p = 0.049$). Interestingly, the Western blot also showed a significant increase in UCH levels for the intermediate ($p = 0.011$) and old age groups ($p = 0.013$) when compared with the youngest age group. The results of the Western blot analyses of the expression of VDAC2 (Fig. 5B) verified a significant increase in the old age group ($p = 0.005$), while also showing increased levels of VDAC2 in the oldest age group ($p = 0.025$) both as compared with the youngest age group. Analyses of the immunoprecipitation of VDAC2 with anti-phosphoserine, anti-phosphothreonine and anti-phosphotyrosine antibodies confirmed a significant decrease in the phosphorylation of VDAC2 in the brain of the NMR for the intermediate age group ($p =$

0.04), the old age group ($p = 0.01$), and in the oldest age group ($p = 0.048$) as compared with the youngest age group (Fig. 5C).

3.3. Evaluation of aspects of autophagy in the NMR with age

To further investigate the role that autophagy (illustrated in Fig. 6) may play in the brain of the NMR with age, the PI3K/Akt/mTOR axis was examined. Western blots were probed for p-PI3K (Tyr⁵⁰⁸), Akt, p-Akt (Ser⁴⁷³), mTOR, and p-mTOR (Ser²⁴⁴⁸) (Fig. 7). Analyses revealed that the p-PI3K protein level was found to be significantly increased from the early to intermediate age group ($p = 0.0001$) and then

Table 1

PDQuest and MS/MS results of NMR brain proteins involved in proteostasis networks with significant altered expression and/or phosphorylation states as a function of age.

Spot	Protein identified	Accession #	Coverage (%)	# of peptides	Score	MW (kDa)	pI	Age groups compared	p-Value expression	Fold change expression	p-Value phosphorylation	Fold change phosphorylation
6205	VDAC1	P21769	36.04	8	39.06	30.8	8.54	1 v 3	–	–	0.0308	0.0132
6203	VDAC2 (Isoform 2)	P45880-2	26.86	7	30.26	30.4	7.20	1 v 2	–	–	0.0004	0.175
								1 v 3	0.0493	44.7	0.0004	0.165
								1 v 4	–	–	0.0008	0.252
7206	VDAC3	Q9Y277	12.01	3	13.86	30.6	8.66	1 v 3	0.0470	10.3	0.0307	0.0470
8106	Proteasome subunit beta type 1	P20618	9.54	2	14.98	26.5	7.20	1 V 2	–	–	0.0133	0.144
								1 v 4	–	–	0.0154	0.199
3804	Ub-like modifier-activating enzyme 1	P22314	12.48	8	32.44	117.8	5.76	1 v 3	–	–	0.0421	42.7
7004	Ub-conjugating enzyme E2 variant 2	Q15819	13.10	2	13.11	16.4	8.09	1 v 2	0.0499	8.83	–	–
								1 v 4	–	–	0.0290	0.0872
3601	Ubiquitin carboxy-terminal hydrolase	A6NJA2	18.53	6	21.49	51.1	5.92	1 v 4	0.0492	18.2	–	–
3604	HSP60	P10809	18.85	9	50.80	61.0	5.87	1 v 2	–	–	0.0359	0.112
2805	HSP70 protein 4	P34932	17.26	11	60.47	94.3	5.19	1 v 3	0.0150	7.72	–	–
								1 v 4	0.0448	6.46	–	–
								2 v 3	0.0417	3.31	–	–

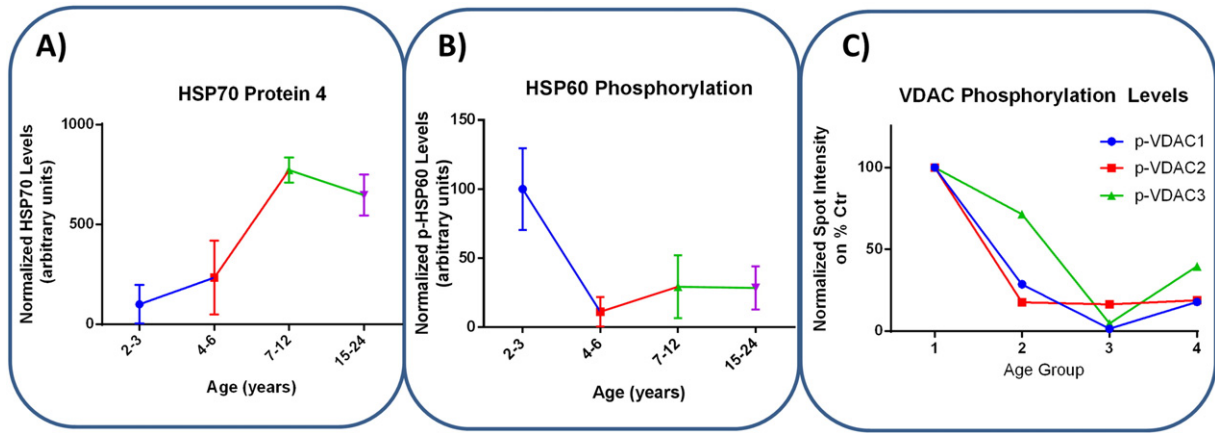


Fig. 3. Linear regressions of selected proteins illustrating trends in median protein levels in NMR brain for: (A) HSP70 protein 4, (B) HSP60, and (C) VDACS 1–3 ($n = 5-9$ individual brains per age group comparison). Data obtained from PDQuest analyses. Spot densities of protein (A) levels were normalized to the total density of the gel by the PDQuest program. Spot densities of phosphorylated (B & C) proteins (labeled by Pro-Q Diamond stain) were normalized to the spot densities of the corresponding spot of the Sypro Ruby-stained gel.

significantly decreased from the intermediate to the old age group ($p = 0.0007$). Additionally, there was a significant decrease from the intermediate to the oldest age group ($p < 0.0001$). The p-Akt/Akt ratio was decreased from the intermediate age group to the old age group ($p = 0.031$). Similar to the other proteins in the PI3K/Akt/mTOR axis, the p-Akt/Akt ratio increases from the youngest to the intermediate age group (data trended toward significance). There were no significant changes in the protein levels of mTOR; however the p-mTOR/mTOR ratio follows a corresponding trend to that of p-PI3K, in which

there is a significant increase from the early to intermediate age group ($p = 0.013$) and a significant decrease from the intermediate age group to the old and oldest age groups ($p = 0.0009$) and ($p = 0.0013$), respectively.

We further analyzed the quantitative index of autophagy, the LC3-II/LC3-I ratio in all age groups. The LC3 ratio showed no significant changes with age (Fig. 8). Additionally, we analyzed levels of the autophagy initiator protein, Beclin-1, which showed a significant decrease in the oldest age group ($p < 0.0001$) (Fig. 8).

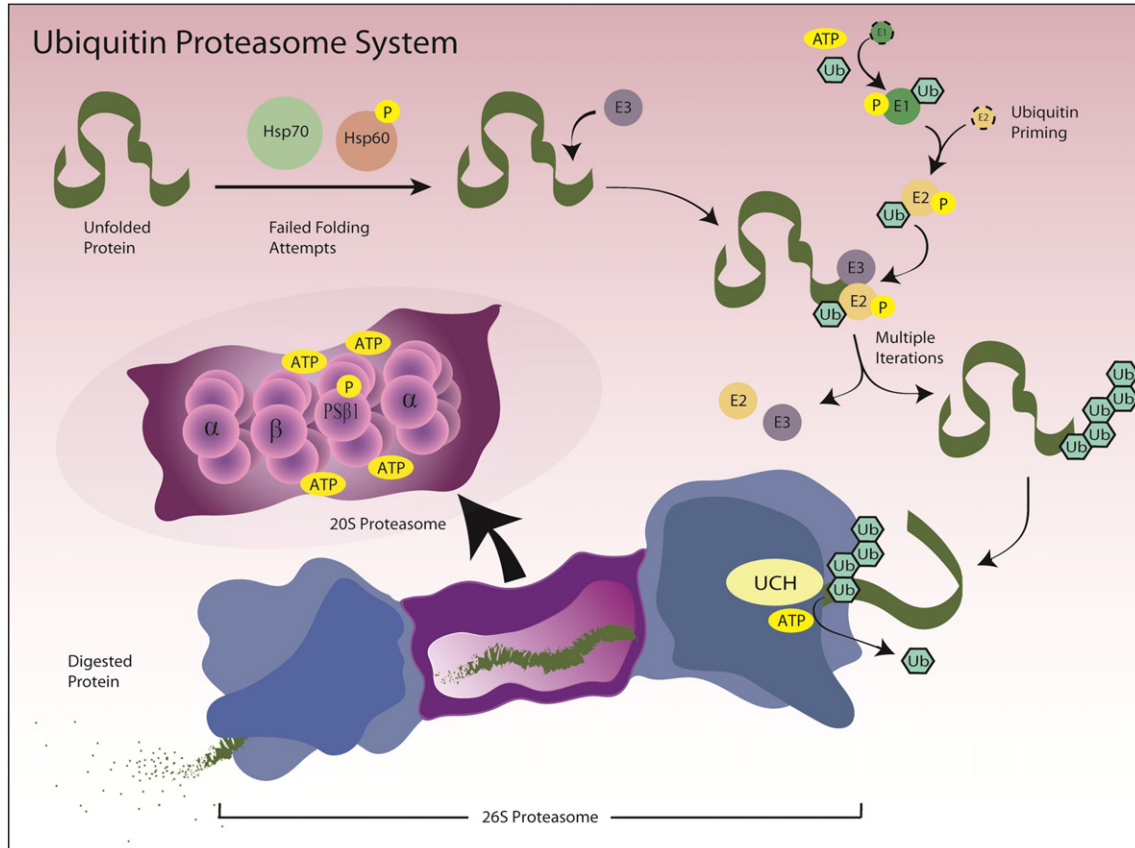


Fig. 4. Summary of schematic diagram of expression proteomics and phosphoproteomics profiles of changes in proteins related to the ubiquitin–proteasomal system in the brain of the NMR as a function of age. Proteins with significantly altered protein and/or phosphorylation levels with age in the NMR brain are labeled.

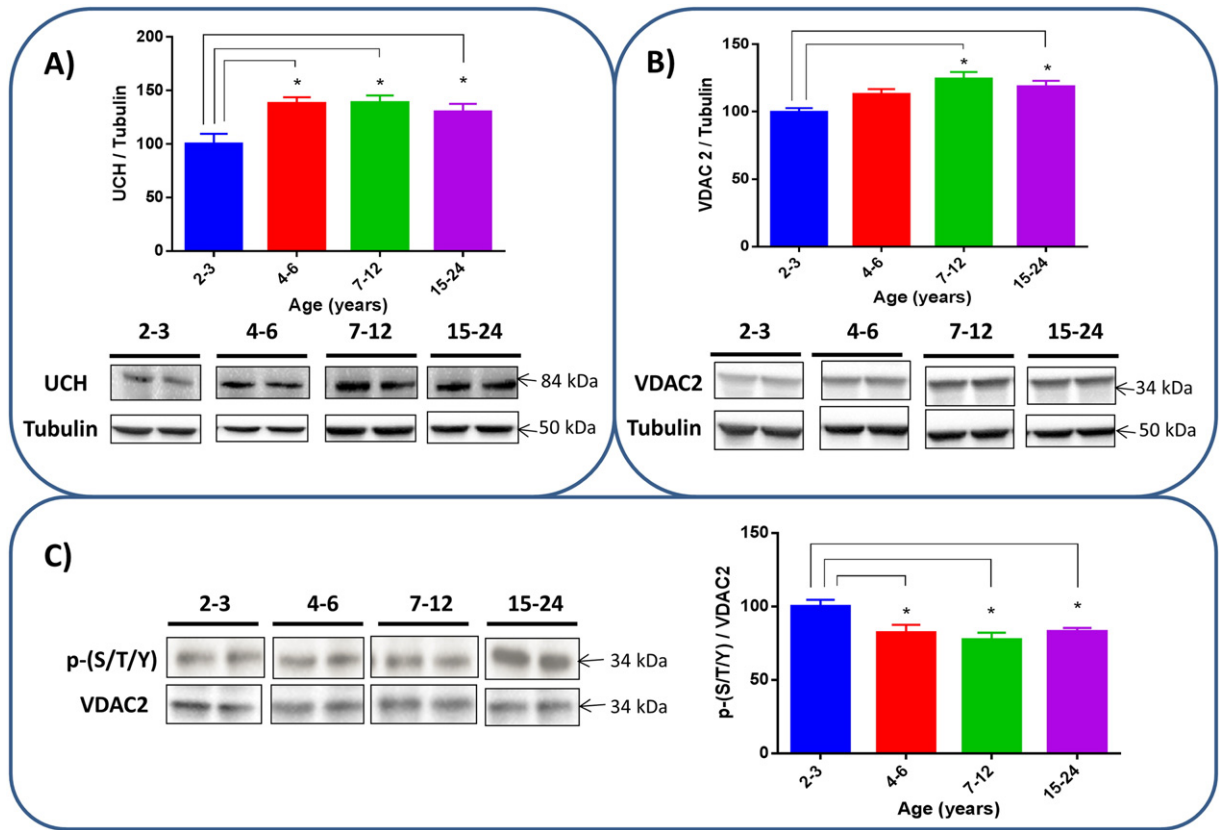


Fig. 5. Western blot and corresponding bar graph representations from the validation experiments of the changes in the protein levels of (A) Ub carboxy-terminal hydrolase (UCH), (B) voltage-dependent anion channel 2 (VDAC2), and (C) the immunocytochemistry experiment validation of the significant decrease (* $p < 0.05$) in the phosphorylation of VDAC2 in the brains of NMRs ($n = 6$ for each age group in A & B; $n = 4$ in C). Immunoreactivity with specific antibodies was detected by chemiluminescence.

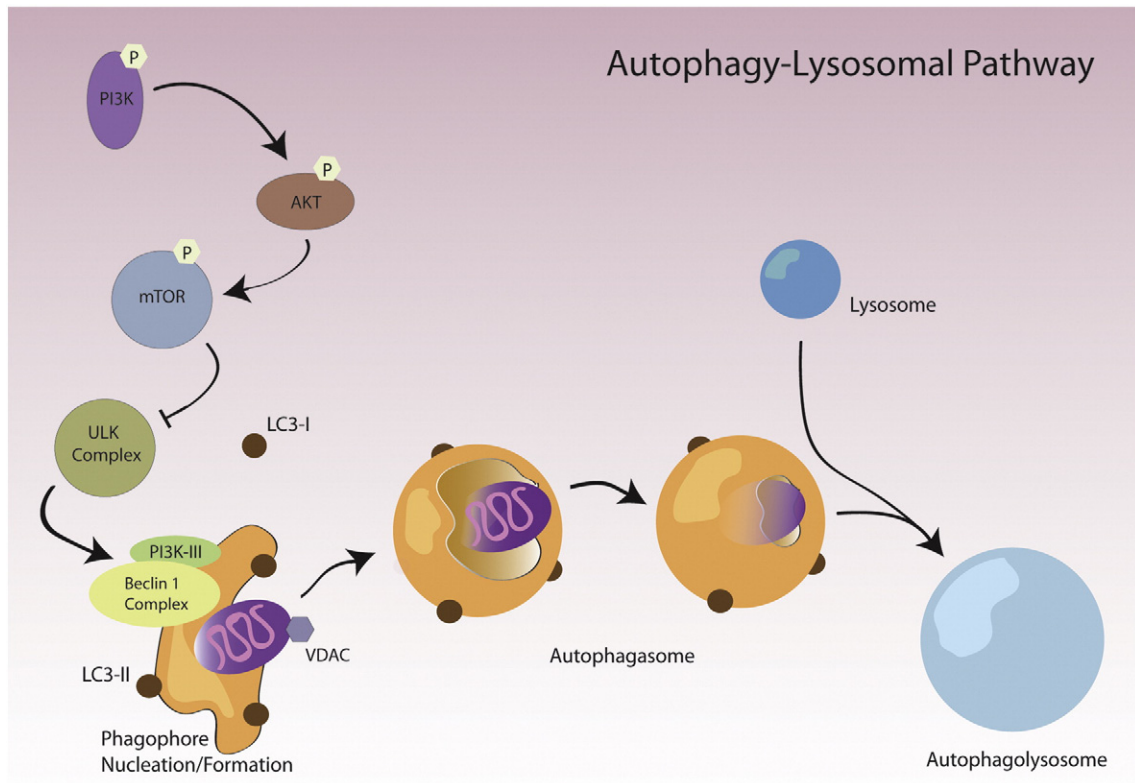


Fig. 6. Diagram summarizing the PI3K/Akt/mTOR axis signaling pathway leading to the nucleation and formation of the phagophore to initiate the autophagy–lysosomal pathway.

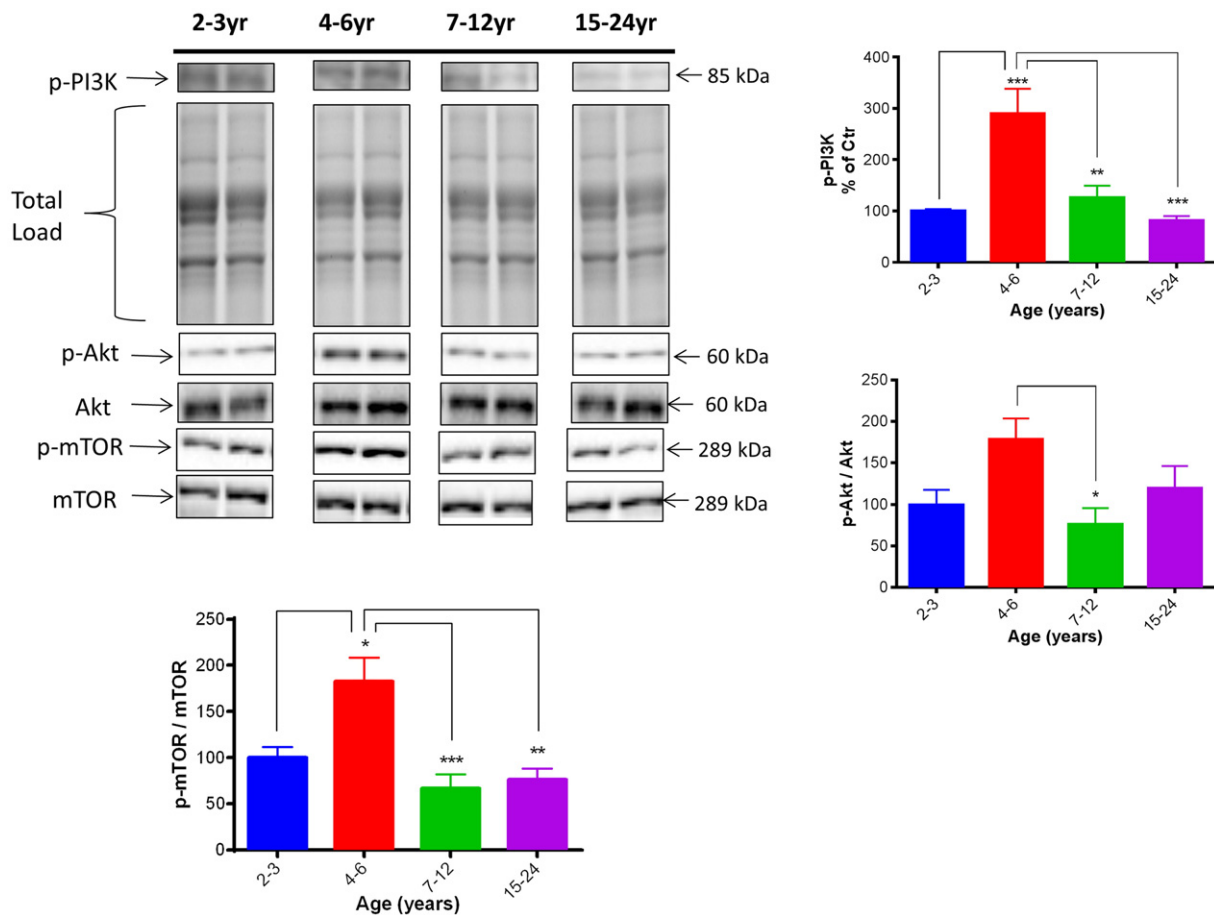


Fig. 7. Western blots and corresponding bar graph representations from the evaluation of the PI3K/Akt/mTOR axis in the brain of the NMR ($n = 6$ for each age group, * $p < 0.05$, ** $p < 0.001$, *** $p < 0.0001$). Phosphorylated PI3K was normalized to the total protein load of each lane of the gel. Phosphorylated Akt and mTOR were normalized to the protein content of Akt and mTOR respectively. Immunoreactivity with specific antibodies was detected by chemiluminescence.

4. Discussion

Not only are NMRs the longest-lived rodent, but they also maintain an extended health span. This extraordinary salubrious lifespan has been attributed to, in part, by mechanisms that contribute to maintaining proteostasis [7]. Processes that promote sustained cellular homeostasis, such as unfolded protein response and proteasome and autophagy pathways, remove damaged or unwanted proteins, macromolecules and organelles which can be cytotoxic and lead to neuronal death [42]. Additionally, these proteostasis systems play a critical role in maintaining health by modulating protein levels in response to fluctuating physiological environments [42]. Previous studies have shown that NMRs exhibit a more robust proteostasis as compared with shorter-lived rodents [7,12–16]. In this current study, we evaluated age-related changes in the NMR proteome and phosphoproteome involved in proteostasis networks. These findings suggest that the NMR is able to maintain this health-sustaining, robust proteostasis throughout the majority of their lifespan. Here, we discuss the implications of proteins with significant differential levels and phosphorylation states from the respective proteomics analyses (Table 1) as well as selected autophagy-related proteins evaluated via Western blot analyses.

Typically, susceptibility to age-related diseases correlates to a declining capacity to generate a stress response [43,44]. Consistent with this notion, in the brain of the salubrious NMR, levels of HSP70 (protein 4) were increased and phosphorylation of HSP60 decreased with age. HSP70 is a highly conserved pleiotropic protein that executes many cellular functions including: folding of newly synthesized proteins, prevention of protein aggregation, aiding in

endocytosis, signal transduction, protein targeting, and relaying proteins to the ubiquitin–proteasome system and autophagy–lysosomal pathways (reviewed in [45]). Moreover, HSP70 mediates proteasome assembly during stress [46], and together with its co-chaperone, HSP40, HSP70 is involved in mitigation of proteotoxic insults to the proteasome [23]. Further, overexpression of HSP70 has been shown to impede apoptotic mechanisms [47,48] and to curtail neurodegeneration and senescence [49,50]. Previously, HSP70 levels in NMRs have been shown to be higher in liver lysates compared with those in mice [23], consistent with the idea that the increased levels of this important chaperone with age in the brain observed in the current study may suggest a more robust and global proteostasis in these long-lived animals.

HSP60 primarily functions in the mitochondria to properly fold proteins. In addition, HSP60 has been reported to have anti-apoptotic properties as it can bind and inhibit pro-apoptotic proteins, Bax and Bak, to prevent neurodegeneration [47,51]. Dephosphorylation of HSP60 has been reported to enhance chaperone functions [52]. Therefore, the data from our current study suggest that HSP60 may contribute to proper mitochondrial function in older NMR brains by preventing protein aggregation and by suppressing apoptotic mechanisms to impede neuronal loss.

Ubiquitylation directs proteins to specific cellular targets, such as proteasomes or DNA, as well as regulating protein interactions and activity [53]. Protein ubiquitylation requires the activation and transfer of Ub to a protein in a three-step process. Two proteins involved in this ubiquitylation process, UBE1 and UBE2v2, were found to have altered levels and/or phosphorylation states in the brains of NMR in different age groups. In the old age group, protein phosphorylation levels of

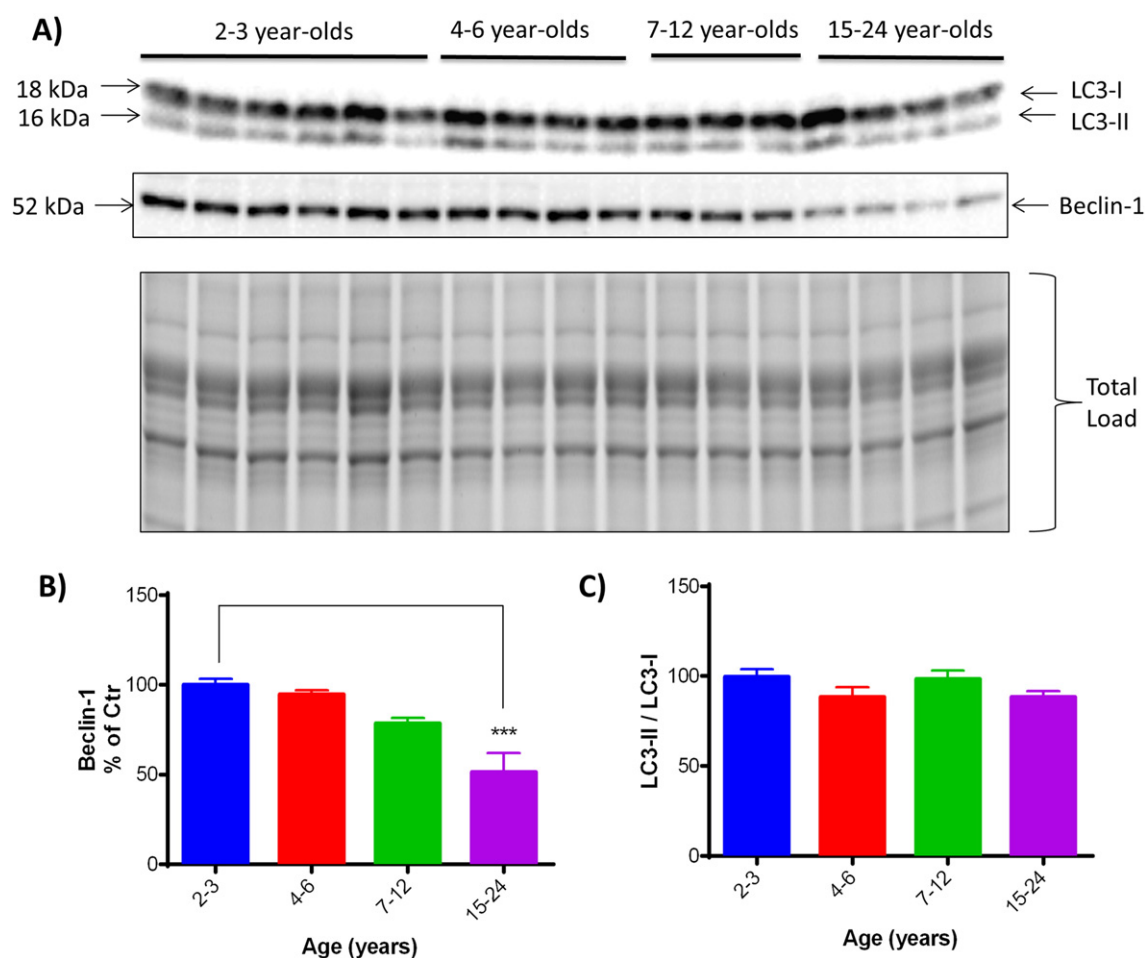


Fig. 8. Western blots and corresponding bar graph representations of Beclin-1 and the LC3-II/LC3-I ratio in the brain of the NMR ($n = 6$ for each age group, $***p < 0.0001$). Proteins were normalized to the total protein load of each lane of the gel. Immunoreactivity with specific antibodies was detected by chemiluminescence.

UBE1 were found to be increased compared with the youngest age group. UBE1 not only catalyzes the first step in the Ub–proteasomal pathway, but it is also essential for the protein ubiquitinylation that modulates DNA double-strand break repair, suggesting an important role in policing genomic integrity and preventing disease pathogenesis [54]. Posttranslational modifications to UBE1 isoforms are still poorly understood [55]. Known putative roles of UBE1 phosphorylation include targeting this protein to different subcellular locations and modulation of nucleotide excision repair [56,57]. However, with multiple UBE1 isoforms containing multiple phosphorylation sites in various domains of the protein, the implications of increased phosphorylation of UBE1 in this current study are as of yet, uncertain. However, as this critical enzyme is reported to be the apex of downstream signaling [55], we opine that UBE1 may be involved in maintaining a healthy genome and conceivably may be related to the dearth of cancer in this long-lived rodent.

Ubiquitinylation is a dynamic process and protein eventual protein destination depends on the lysine to which it is attached and whether it is monoubiquitinylated, homo-polyubiquitinylated, or hetero-polyubiquitinylated [58,59]. The UBE2v2 preferentially ubiquitinylates Lys63, which is reported to participate in chaperoning proteins for DNA repair, lysosomal degradation of epidermal growth factor receptors, and NF- κ B activation by degradation of class I major histocompatibility complex molecules [60–63]. Here, protein levels of UBE2v2 were increased in the intermediate age group, while phosphorylation levels were decreased in the intermediate and oldest age groups. The intricacies of UBE2 structure and function are complex; and as such, the implications of altered phosphorylation states have yet to be

elucidated, though we speculate that this protein may be involved in promoting the ability for NMR to maintain a healthy genome.

UCHs are a family of proteins responsible for the removal of the poly-Ub tags. Dysregulation of UCH may result in the accumulation of poly-Ub proteins; and this accumulation is reported in many chronic neurodegenerative diseases, as they are present in the senile plaques and neurofibrillary tangles in Alzheimer's disease (AD) and in the Lewy bodies of Parkinson's disease [64]. Further, in AD, it is hypothesized that the UPS-mediated degradation of amyloid-beta ($A\beta$) is impaired, which leads to ubiquitinylated $A\beta$ aggregating into neurotoxic plaques [65]. Previously, we have shown that a particular UCH variant, UCHL1, is oxidized in AD brain, which could conceivably inhibit $A\beta$ degradation [66,67]. However, it has been reported that even though NMRs exhibit $A\beta$ levels similar to that of 3xTg-AD mice, there is no accumulation of senile plaques in the NMR brain [8,68]. Moreover, in mice ubiquitinylated proteins accumulate with age; however, in NMRs levels of ubiquitinylated proteins of 2 year-old and 26 year-old rodents were similar [12]. Therefore, the increase of UCH levels in the brain of the oldest age group may function to maintain prolonged cellular proteostasis via availability to mediate disposal of increasing levels of neurotoxic proteins, such as $A\beta$.

When attached to the 26S proteasome and after the removal of Ub by UCH, the protein is degraded by threonine proteases in the core of the 26S proteasome [69]. In this current study, PS β 1, which is responsible for PGPH activity, was found to have decreased levels of phosphorylation in the intermediate and oldest age groups as compared with the youngest age group. Decreases in proteasomal function and/or expression have been reported in multiple neurodegenerative diseases including: AD,

PD, Huntington disease, amyotrophic lateral sclerosis, and prion diseases [70–74]. Moreover, β 1, the variant identified in this current study, has been reported to promote anti-apoptotic activity of plasminogen activator inhibitor 2 (PAI2) [75]. While the consequences of the phosphorylation of this subunit are unclear, it has been shown that phosphorylation of β -subunits in the prokaryote *Myobacterium tuberculosis* can inhibit proteasomal assembly [76]. While there are multiple β -subunits in eukaryotes, unlike in prokaryotes that have only one type, the reduced phosphorylated states in the oldest NMR brains could suggest that there is an increased affinity toward proteome assembly and therefore, an increased degradation of unwanted or damaged proteins, clearing the cell of detritus to promote healthy cellular function. This observation would be consistent with the observed high levels of proteasome activity reported for brain lysates of the NMR [8].

Voltage dependent anion channels (VDACs) are outer mitochondrial membrane porins that are involved in mitochondrial metabolic processes by opening at low membrane potentials to regulate metabolic flux of small hydrophilic molecules and ions [77,78]. VDACs also participate in mitochondrial autophagy by recruiting Parkin to docking sites for the removal of defective mitochondria, targeting the organelle for degradation by lysosomes [79–81]. Decreased levels of VDACs could lead to an increased presence of malfunctioning mitochondria, leading to increased protein oxidation and cellular detritus and ensuing neuronal dysregulation. However, in this study, the increased levels of VDACs suggest that the metabolic flux and the policing of mitochondrial function are improved in the aging brain of the NMR. VDACs are known to be phosphorylated by multiple kinases including: PKA, GSK3 β , PKC, p38 MAP kinase, Nek1, and endostatin reduced hexokinase 2 [81,82]. Phosphorylation of VDAC1 by Nek1 has been reported to open the channel [82]. VDAC phosphorylation by GSK3 β or PKA increases the interaction between VDAC and tubulin, blocking the channel [81]. The consequences of the decreased phosphorylation levels of VDAC2 and VDAC3 in the aged NMR brain are unclear and may reflect the greater proportion of breeding animals in the older samples. Further investigations are needed to elucidate the implications of this reported global decrease in phosphorylation in brains of NMR rodents with age.

To further assess the role that autophagy may contribute to the sustained health span of the NMR by regulating cellular proteostasis, the PI3K/Akt/mTOR axis, Beclin-1 and LC3 were examined in the NMR brain as a function of age. Previous data suggested that the NMR, under basal conditions, maintains higher levels of autophagy, thereby removing potentially toxic proteins before they can negatively impact organ functionality [13] and that macroautophagy was shown to be substantially higher in NMRs than in shorter-lived mice [13,16]. Further, when the autophagy markers LC3-I, LC3-II and Beclin-1 were measured in one-day-old NMRs and one-day-old mice, the NMRs were shown to have a higher LC3-II/LC3-I ratio, even though their Beclin-1 levels were lower, suggesting that NMRs have significantly higher basal levels of autophagy than mice [7]. Although Beclin-1 plays a critical role in the regulation of autophagosome formation, it is also a shorter-lived protein involved in the formation of pre-autophagosomal structures. Consequently, it is generally accepted that the LC3-II/LC3-I levels usually correlate more reliably with the number of autophagosomes and can be used to monitor autophagosome formation [83]. Here, we measured the levels of Beclin-1 in the brain of the NMR as a function of age. Beclin-1 was significantly decreased in the oldest age group relative to the youngest age group. When the LC3-II/LC3-I ratio was measured, the levels of this quantitative index of autophagy did not significantly change, suggesting that NMRs do maintain a high level of autophagy throughout a vast majority of their lives.

The serine/threonine kinase, mTOR, is a major modulator of autophagy that receives inputs from many different signaling pathways [84]. One of the most important upstream positive regulators of mTOR is Akt. The hyperphosphorylation of Akt induces a complete inhibition of

TSC2 and activation of mTOR through direct phosphorylation. In turn, the mechanism of activation of Akt is induced by another kinase, PI3K. All together, these proteins are recognized as the PI3K/Akt/mTOR axis, which plays a central role in controlling one of the processes of proteostasis, autophagy. Our results showed increased phosphorylation of Akt and PI3K (p85 subunit) at Ser⁴⁷³ and Tyr⁵⁰⁸, respectively, in the intermediate NMR age group. This group was made up predominantly of breeding pairs and the unexpected change in this group likely indicates that breeding status may affect mTOR signaling through the interaction of the pathway with sex steroids. The hyperphosphorylation of these two proteins do not appear to affect NMR aging negatively. Indeed, the increase of PI3K/Akt activity in intermediate-aged NMRs in this study could reflect the diversity of one of the several main downstream targets, mTOR. Consistent with this notion, our data showed a hyperphosphorylation of mTOR at Ser²⁴⁴⁸ in the brain of this age cohort. Additionally, an increase in activity of the proteasome was noted by a decrease in phosphorylation of PS β 1 for the intermediate age group (Table 1), perhaps as a compensatory mechanism to the decreased autophagic response seen in this age group.

Taken together, these results demonstrate a plausible mechanism by which NMRs resist development of age-related diseases, even though they show high levels of oxidative damage to visceral tissues, even at young ages [10,85]. Given that NMRs endogenously produce high levels of A β and phosphorylated tau at a young age, yet live more than two decades with these high levels, it appears that this species is exceedingly tolerant of high levels of these proteins reportedly casually associated with Alzheimer's disease and has evolved mechanisms to counter its neurotoxicity [8,68,86]. One possible explanation could be the sustained activity of the autophagy pathway in the older age groups. In fact, a recent paper published from our lab, supporting earlier findings by LaFerla, Oddo and others, showed increased activity of the autophagy pathway in AD and Down syndrome subjects, suggesting that A β could be one of the major causes causing hyperactivation of the pathway [86].

Brains used in this study were obtained from NMR animals which were both male and female breeding and non-breeding animals. Consequently, a possible caveat of these results may be sample variation due to breeding status and resultant hormonal differences [87]. To assess the contribution of breeding status, future studies comprising a larger number of NMRs of both breeding and non-breeding status will be necessary. Understanding and characterizing the contributions of breeding status to the NMR proteome are essential to clarify this potential caveat of the current and many prior NMR studies.

Our results of this age-related study in the brain of the NMR expose significant alterations in protein levels and phosphorylation states of proteins involved in the functioning of the proteostasis network. In general, the identified proteins and phosphoproteins tend to have increased expression and/or activity that promote proteostasis. Mechanisms that remove cellular detritus promote an efficient, functional environment. Additionally, by using long-lived species to identify specific proteins involved in these processes, targets for potential therapies are identified that conceivably may aid in increasing human health span.

Transparency document

The [Transparency document](#) associated with this article can be found, in the online version.

References

- [1] V. Gorbunova, A. Seluanov, Z. Zhang, V.N. Gladyshev, J. Vijg, Comparative genetics of longevity and cancer: insights from long-lived rodents, *Nat. Rev. Genet.* 15 (2014) 531–540.
- [2] E.B. Kim, X. Fang, A.A. Fushan, Z. Huang, A.V. Lobanov, L. Han, S.M. Marino, X. Sun, A.A. Turanov, P. Yang, S.H. Yim, X. Zhao, M.V. Kasaikina, N. Stoletzki, C. Peng, P. Polak, Z. Xiong, A. Kiezun, Y. Zhu, Y. Chen, G.V. Kryukov, Q. Zhang, L. Peshkin, L. Yang, R.T. Bronson, R. Buffenstein, B. Wang, C. Han, Q. Li, L. Chen, W. Zhao, S.R. Sunyaev, T.J. Park, G. Zhang, J. Wang, V.N. Gladyshev, Genome sequencing reveals

- insights into physiology and longevity of the naked mole rat, *Nature* 479 (2011) 223–227.
- [3] R. Buffenstein, The naked mole-rat: a new long-living model for human aging research, *J. Gerontol. A: Biol. Med. Sci.* 60 (2005) 1369–1377.
 - [4] Y.H. Edrey, M. Hanes, M. Pinto, J. Mele, R. Buffenstein, Successful aging and sustained good health in the naked mole rat: a long-lived mammalian model for biogerontology and biomedical research, *ILAR J.* 52 (2011) 41–53.
 - [5] R. Buffenstein, Negligible senescence in the longest living rodent, the naked mole-rat: insights from a successfully aging species, *J. Comp. Physiol. B.* 178 (2008) 439–445.
 - [6] G.P. Ables, H.M. Brown-Borg, R. Buffenstein, C.D. Church, A.K. Elshorbagy, V.N. Gladyshev, T.H. Huang, R.A. Miller, J.R. Mitchell, J.P. Richie, B. Rogina, M.H. Stipanuk, D.S. Orentreich, N. Orentreich, The first international mini-symposium on methionine restriction and lifespan, *Front. Genet.* 5 (2014) 122.
 - [7] S. Zhao, L. Lin, G. Kan, C. Xu, Q. Tang, C. Yu, W. Sun, L. Cai, C. Xu, S. Cui, High autophagy in the naked mole rat may play a significant role in maintaining good health, *Cell. Physiol. Biochem.* 33 (2014) 321–332.
 - [8] Y.H. Edrey, S. Oddo, C. Cornelius, A. Caccamo, V. Calabrese, R. Buffenstein, Oxidative damage and amyloid-beta metabolism in brain regions of the longest-lived rodents, *J. Neurosci. Res.* 92 (2014) 195–205.
 - [9] K.N. Lewis, B. Andziak, T. Yang, R. Buffenstein, The naked mole-rat response to oxidative stress: just deal with it, *Antioxid. Redox Signal.* 19 (2013) 1388–1399.
 - [10] B. Andziak, T.P. O'Connor, W. Qi, E.M. DeWaal, A. Pierce, A.R. Chaudhuri, H. Van Remmen, R. Buffenstein, High oxidative damage levels in the longest-living rodent, the naked mole-rat, *Aging Cell* 5 (2006) 463–471.
 - [11] A.J. Lambert, H.M. Boysen, J.A. Buckingham, T. Yang, A. Podlutzky, S.N. Austad, T.H. Kunz, R. Buffenstein, M.D. Brand, Low rates of hydrogen peroxide production by isolated heart mitochondria associate with long maximum lifespan in vertebrate homeotherms, *Aging Cell* 6 (2007) 607–618.
 - [12] V.I. Perez, R. Buffenstein, V. Masamsetti, S. Leonard, A.B. Salmon, J. Mele, B. Andziak, T. Yang, Y. Edrey, B. Friguet, W. Ward, A. Richardson, A. Chaudhuri, Protein stability and resistance to oxidative stress are determinants of longevity in the longest-living rodent, the naked mole-rat, *Proc. Natl. Acad. Sci. U. S. A.* 106 (2009) 3059–3064.
 - [13] K.A. Rodriguez, E. Wywiał, V.I. Perez, A.J. Lambert, Y.H. Edrey, K.N. Lewis, K. Grimes, M.L. Lindsey, M.D. Brand, R. Buffenstein, Walking the oxidative stress tightrope: a perspective from the naked mole-rat, the longest-living rodent, *Curr. Pharm. Des.* 17 (2011) 2290–2307.
 - [14] K.A. Rodriguez, Y.H. Edrey, P. Osmulski, M. Gaczynska, R. Buffenstein, Altered composition of liver proteasome assemblies contributes to enhanced proteasome activity in the exceptionally long-lived naked mole-rat, *PLoS ONE* 7 (2012) e35890.
 - [15] K. Grimes, Y. Chiao, M.L. Lindsey, R. Buffenstein, Cardiac function in an extraordinarily long-lived rodent, the naked mole-rat, *Circulation* 126 (2012).
 - [16] H. Pride, Z. Yu, B. Sunchu, J. Mochnick, A. Coles, Y. Zhang, R. Buffenstein, P.J. Hornsby, S.N. Austad, V.I. Pérez, Long-lived species have improved proteostasis compared to phylogenetically-related shorter-lived species, *Biochem. Biophys. Res. Commun.* 457 (2015) 669–675.
 - [17] E. Leroy, R. Boyer, G. Auburger, B. Leube, G. Ulm, E. Mezey, G. Harta, M.J. Brownstein, S. Jonnalagada, T. Chernova, A. Dehejia, C. Lavedan, T. Gasser, P.J. Steinbach, K.D. Wilkinson, M.H. Polymeropoulos, The ubiquitin pathway in Parkinson's disease, *Nature* 395 (1998) 451–452.
 - [18] P. Fernandez-Funez, M.L. Nino-Rosales, B. de Gouyon, W.C. She, J.M. Luchak, P. Martinez, E. Turiegano, J. Benito, M. Capovilla, P.J. Skinner, A. McCall, I. Canal, H.T. Orr, H.Y. Zoghbi, J. Botas, Identification of genes that modify ataxin-1-induced neurodegeneration, *Nature* 408 (2000) 101–106.
 - [19] A. Castegna, V. Thongboonkerd, J. Klein, B.C. Lynn, Y.L. Wang, H. Osaka, K. Wada, D.A. Butterfield, Proteomic analysis of brain proteins in the fragile axonal dystrophy (gad) mouse, a syndrome that emanates from dysfunctional ubiquitin carboxyl-terminal hydrolase L-1, reveals oxidation of key proteins, *J. Neurochem.* 88 (2004) 1540–1546.
 - [20] J. Triplett, Z. Zhang, R. Sultana, J. Cai, J.B. Klein, H. Bueler, D.A. Butterfield, Quantitative expression proteomics and phosphoproteomics profile of brain from PINK1 knock-out mice: insights into mechanisms of familial Parkinson disease, *J. Neurochem.* 133 (2015) 750–765.
 - [21] E.J. Bennett, T.A. Shaler, B. Woodman, K.Y. Ryu, T.S. Zaitseva, C.H. Becker, G.P. Bates, H. Schulman, R.R. Kopito, Global changes to the ubiquitin system in Huntington's disease, *Nature* 448 (2007) 704–708.
 - [22] J. Hanna, D. Finley, A proteasome for all occasions, *FEBS Lett.* 581 (2007) 2854–2861.
 - [23] K.A. Rodriguez, P.A. Osmulski, A. Pierce, S.T. Weintraub, M. Gaczynska, R. Buffenstein, A cytosolic protein factor from the naked mole-rat activates proteasomes of other species and protects these from inhibition, *Biochim. Biophys. Acta* 1842 (2014) 2060–2072.
 - [24] N. Mizushima, Autophagy: process and function, *Genes Dev.* 21 (2007) 2861–2873.
 - [25] F. Cecconi, B. Levine, The role of autophagy in mammalian development: cell make-over rather than cell death, *Dev. Cell* 15 (2008) 344–357.
 - [26] D.J. Klionsky, The molecular machinery of autophagy: unanswered questions, *J. Cell Sci.* 118 (2005) 7–18.
 - [27] D. Glick, S. Barth, K.F. Macleod, Autophagy: cellular and molecular mechanisms, *J. Pathol.* 221 (2010) 3–12.
 - [28] A.R. Winslow, C.W. Chen, S. Corrochano, A. Acevedo-Arozena, D.E. Gordon, A.A. Peden, M. Lichtenberg, F.M. Menzies, B. Ravikumar, S. Imarisio, S. Brown, C.J. O'Kane, D.C. Rubinsztein, Alpha-synuclein impairs macroautophagy: implications for Parkinson's disease, *J. Cell Biol.* 190 (2010) 1023–1037.
 - [29] M. Martinez-Vicente, Z. Talloczy, E. Wong, G. Tang, H. Koga, S. Kaushik, R. de Vries, E. Arias, S. Harris, D. Sulzer, A.M. Cuervo, Cargo recognition failure is responsible for inefficient autophagy in Huntington's disease, *Nat. Neurosci.* 13 (2010) 567–576.
 - [30] C. Aguado, S. Sarkar, V.I. Korolchuk, O. Criado, S. Vernia, P. Boya, P. Sanz, S.R. de Cordoba, E. Knecht, D.C. Rubinsztein, Laforin, the most common protein mutated in Lafora disease, regulates autophagy, *Hum. Mol. Genet.* 19 (2010) 2867–2876.
 - [31] R.A. Nixon, D.S. Yang, Autophagy failure in Alzheimer's disease—locating the primary defect, *Neurobiol. Dis.* 43 (2011) 38–45.
 - [32] R.A. Nixon, The role of autophagy in neurodegenerative disease, *Nat. Med.* 19 (2013) 983–997.
 - [33] A. Tramutola, J. Triplett, F.D. Domenico, D.M. Niedowicz, M.P. Murphy, R. Coccia, M. Perluigi, D.A. Butterfield, Alteration of mTOR signaling occurs early in the progression of Alzheimer disease: analysis of brain from subjects with Preclinical AD, amnesic mild cognitive impairment and late-stage AD, *J. Neurochem.* 133 (2015) 739–749.
 - [34] S. Grimm, A. Hoehn, K.J. Davies, T. Grune, Protein oxidative modifications in the ageing brain: consequence for the onset of neurodegenerative disease, *Free Radic. Res.* 45 (2011) 73–88.
 - [35] K. Willeumier, S.M. Pulst, F.E. Schweizer, Proteasome inhibition triggers activity-dependent increase in the size of the recycling vesicle pool in cultured hippocampal neurons, *J. Neurosci. Off. J. Soc. Neurosci.* 26 (2006) 11333–11341.
 - [36] J.J. Yi, M.D. Ehlers, Emerging roles for ubiquitin and protein degradation in neuronal function, *Pharmacol. Rev.* 59 (2007) 14–39.
 - [37] K. Tanaka, N. Matsuda, Proteostasis and neurodegeneration: the roles of proteasomal degradation and autophagy, *Biochim. Biophys. Acta* 1843 (2014) 197–204.
 - [38] P.K. Smith, R.I. Krohn, G.T. Hermanson, A.K. Mallia, F.H. Gartner, M.D. Provenzano, E.K. Fujimoto, N.M. Goeke, B.J. Olson, D.C. Klenk, Measurement of protein using bicinchoninic acid, *Anal. Biochem.* 150 (1985) 76–85.
 - [39] R. Sultana, D. Boyd-Kimball, J. Cai, W.M. Pierce, J.B. Klein, M. Merchant, D.A. Butterfield, Proteomics analysis of the Alzheimer's disease hippocampal proteome, *J. Alzheimers Dis.* 11 (2007) 153–164.
 - [40] F. Di Domenico, R. Sultana, E. Barone, M. Perluigi, C. Cini, C. Mancuso, J. Cai, W.M. Pierce, D.A. Butterfield, Quantitative proteomics analysis of phosphorylated proteins in the hippocampus of Alzheimer's disease subjects, *J. Proteome* 74 (2011) 1091–1103.
 - [41] V. Thongboonkerd, K.R. McLeish, J.M. Arthur, J.B. Klein, Proteomic analysis of normal human urinary proteins isolated by acetone precipitation or ultracentrifugation, *Kidney Int.* 62 (2002) 1461–1469.
 - [42] F. Di Domenico, E. Head, D.A. Butterfield, M. Perluigi, Oxidative stress and proteostasis network: culprit and casualty of Alzheimer's-like neurodegeneration, *Adv. Geriatr.* 2014 (2014) 14.
 - [43] R. Njemini, M.V. Abeele, C. Demanet, M. Lambert, S. Vandebosch, T. Mets, Age-related decrease in the inducibility of heat-shock protein 70 in human peripheral blood mononuclear cells, *J. Clin. Immunol.* 22 (2002) 195–205.
 - [44] A. Gutschmann-Conrad, A.R. Heydari, S. You, A. Richardson, The expression of heat shock protein 70 decreases with cellular senescence in vitro and in cells derived from young and old human subjects, *Exp. Cell Res.* 241 (1998) 404–413.
 - [45] E. Meimaridou, S.B. Gooljar, J.P. Chapple, From hatching to dispatching: the multiple cellular roles of the Hsp70 molecular chaperone machinery, *J. Mol. Endocrinol.* 42 (2009) 1–9.
 - [46] T. Grune, B. Catalgol, A. Licht, G. Ermak, A.M. Pickering, J.K. Ngo, K.J. Davies, HSP70 mediates dissociation and reassociation of the 26S proteasome during adaptation to oxidative stress, *Free Radic. Biol. Med.* 51 (2011) 1355–1364.
 - [47] R. Arya, M. Mallik, S.C. Lakhota, Heat shock genes – integrating cell survival and death, *J. Biosci.* 32 (2007) 595–610.
 - [48] M.P. Mayer, B. Bukau, Hsp70 chaperones: cellular functions and molecular mechanism, *Cell. Mol. Life Sci.* 62 (2005) 670–684.
 - [49] N.M. Bonini, Chaperoning brain degeneration, *Proc. Natl. Acad. Sci. U. S. A.* 99 (Suppl. 4) (2002) 16407–16411.
 - [50] J. Klucken, Y. Shin, E. Masliash, B.T. Hyman, P.J. McLean, Hsp70 reduces alpha-synuclein aggregation and toxicity, *J. Biol. Chem.* 279 (2004) 25497–25502.
 - [51] D. Chandra, G. Choy, D.G. Tang, Cytosolic accumulation of HSP60 during apoptosis with or without apparent mitochondrial release: evidence that its pro-apoptotic or pro-survival functions involve differential interactions with caspase-3, *J. Biol. Chem.* 282 (2007) 31289–31301.
 - [52] I.U. Khan, R. Wallin, R.S. Gupta, G.M. Kammer, Protein kinase A-catalyzed phosphorylation of heat shock protein 60 chaperone regulates its attachment to histone 2B in the T lymphocyte plasma membrane, *Proc. Natl. Acad. Sci. U. S. A.* 95 (1998) 10425–10430.
 - [53] Y. David, T. Ziv, A. Admon, A. Navon, The E2 ubiquitin-conjugating enzymes direct polyubiquitination to preferred lysines, *J. Biol. Chem.* 285 (2010) 8595–8604.
 - [54] P. Moudry, C. Lukas, L. Macurek, H. Hanzlikova, Z. Hodny, J. Lukas, J. Bartek, Ubiquitin-activating enzyme UBA1 is required for cellular response to DNA damage, *Cell Cycle* 11 (2012) 1573–1582.
 - [55] B.A. Schulman, J.W. Harper, Ubiquitin-like protein activation by E1 enzymes: the apex for downstream signalling pathways, *Nat. Rev. Mol. Cell Biol.* 10 (2009) 319–331.
 - [56] A.G. Stephen, J.S. Trausch-Azar, A. Ciechanover, A.L. Schwartz, The ubiquitin-activating enzyme E1 is phosphorylated and localized to the nucleus in a cell cycle-dependent manner, *J. Biol. Chem.* 271 (1996) 15608–15614.
 - [57] T. Nospikel, P.C. Hanawalt, Impaired nucleotide excision repair upon macrophage differentiation is corrected by E1 ubiquitin-activating enzyme, *Proc. Natl. Acad. Sci. U. S. A.* 103 (2006) 16188–16193.
 - [58] F. Shang, G. Deng, Q. Liu, W. Guo, A.L. Haas, B. Crosas, D. Finley, A. Taylor, Lys6-modified ubiquitin inhibits ubiquitin-dependent protein degradation, *J. Biol. Chem.* 280 (2005) 20365–20374.
 - [59] E.S. Johnson, P.C. Ma, I.M. Ota, A. Varshavsky, A proteolytic pathway that recognizes ubiquitin as a degradation signal, *J. Biol. Chem.* 270 (1995) 17442–17456.

- [60] R.M. Hofmann, C.M. Pickart, Noncanonical MMS2-encoded ubiquitin-conjugating enzyme functions in assembly of novel polyubiquitin chains for DNA repair, *Cell* 96 (1999) 645–653.
- [61] L.M. Duncan, S. Piper, R.B. Dodd, M.K. Saville, C.M. Sanderson, J.P. Luzio, P.J. Lehner, Lysine-63-linked ubiquitination is required for endolysosomal degradation of class I molecules, *EMBO J.* 25 (2006) 1635–1645.
- [62] F. Huang, D. Kirkpatrick, X. Jiang, S. Gygi, A. Sorkin, Differential regulation of EGF receptor internalization and degradation by multiubiquitination within the kinase domain, *Mol. Cell* 21 (2006) 737–748.
- [63] C.J. Wu, D.B. Conze, T. Li, S.M. Srinivasula, J.D. Ashwell, Sensing of Lys 63-linked polyubiquitination by NEMO is a key event in NF-kappaB activation [corrected], *Nat. Cell Biol.* 8 (2006) 398–406.
- [64] A.L. Schwartz, A. Ciechanover, The ubiquitin–proteasome pathway and pathogenesis of human diseases, *Annu. Rev. Med.* 50 (1999) 57–74.
- [65] L. Hong, H.-C. Huang, Z.-F. Jiang, Relationship between amyloid-beta and the ubiquitin–proteasome system in Alzheimer's disease, *Neurol. Res.* 36 (2014) 276–282.
- [66] A. Castegna, M. Aksenov, M. Aksenova, V. Thongboonkerd, J.B. Klein, W.M. Pierce, R. Booze, W.R. Markesbery, D.A. Butterfield, Proteomic identification of oxidatively modified proteins in Alzheimer's disease brain. Part I: creatine kinase BB, glutamine synthase, and ubiquitin carboxy-terminal hydrolase L-1, *Free Radic. Biol. Med.* 33 (2002) 562–571.
- [67] R. Sultana, D. Boyd-Kimball, H.F. Poon, J. Cai, W.M. Pierce, J.B. Klein, M. Merchant, W.R. Markesbery, D.A. Butterfield, Redox proteomics identification of oxidized proteins in Alzheimer's disease hippocampus and cerebellum: an approach to understand pathological and biochemical alterations in AD, *Neurobiol. Aging* 27 (2006) 1564–1576.
- [68] Y.H. Edrey, D.X. Medina, M. Gaczynska, P.A. Osmulski, S. Oddo, A. Caccamo, R. Buffenstein, Amyloid beta and the longest-lived rodent: the naked mole-rat as a model for natural protection from Alzheimer's disease, *Neurobiol. Aging* 34 (2013) 2352–2360.
- [69] D. Voges, P. Zwickl, W. Baumeister, The 26S proteasome: a molecular machine designed for controlled proteolysis, *Annu. Rev. Biochem.* 68 (1999) 1015–1068.
- [70] D. Ebrahimi-Fakhari, L. Wahlster, P. McLean, Protein degradation pathways in Parkinson's disease: curse or blessing, *Acta Neuropathol.* 124 (2012) 153–172.
- [71] S. Bukhatwa, B.-Y. Zeng, S. Rose, P. Jenner, A comparison of changes in proteasomal subunit expression in the substantia nigra in Parkinson's disease, multiple system atrophy and progressive supranuclear palsy, *Brain Res.* 1326 (2010) 174–183.
- [72] D. Martins-Branco, A.R. Esteves, D. Santos, D.M. Arduino, R.H. Swerdlow, C.R. Oliveira, C. Janeiro, S.M. Cardoso, Ubiquitin proteasome system in Parkinson's disease: a keeper or a witness? *Exp. Neurol.* 238 (2012) 89–99.
- [73] J.N. Keller, K.B. Hanni, W.R. Markesbery, Impaired proteasome function in Alzheimer's disease, *J. Neurochem.* 75 (2000) 436–439.
- [74] A. Ciechanover, P. Brundin, The ubiquitin proteasome system in neurodegenerative diseases: sometimes the chicken, sometimes the egg, *Neuron* 40 (2003) 427–446.
- [75] J. Fan, Y.Q. Zhang, P. Li, M. Hou, L. Tan, X. Wang, Y.S. Zhu, Interaction of plasminogen activator inhibitor-2 and proteasome subunit, beta type 1, *Acta Biochim. Biophys. Sin.* 36 (2004) 42–46.
- [76] T. Anandan, J. Han, H. Baun, S. Nyayapathy, J.T. Brown, R.L. Dial, J.A. Moltalvo, M.S. Kim, S.H. Yang, D.R. Ronning, R.N. Husson, J. Suh, C.M. Kang, Phosphorylation regulates mycobacterial proteasome, *J. Microbiol.* 52 (2014) 743–754.
- [77] E. Blachly-Dyson, M. Forte, VDACC channels, *IUBMB Life* 52 (2001) 113–118.
- [78] V. Shoshan-Barmatz, D. Gincel, The voltage-dependent anion channel, *Cell Biochem. Biophys.* 39 (2003) 279–292.
- [79] Y. Sun, A.A. Vashisht, J. Tchiew, J.A. Wohlschlegel, L. Dreier, Voltage-dependent anion channels (VDACCs) recruit Parkin to defective mitochondria to promote mitochondrial autophagy, *J. Biol. Chem.* 287 (2012) 40652–40660.
- [80] S. Geisler, K.M. Holmstrom, D. Skujat, F.C. Fiesel, O.C. Rothfuss, P.J. Kahle, W. Springer, PINK1/Parkin-mediated mitophagy is dependent on VDACC1 and p62/SQSTM1, *Nat. Cell Biol.* 12 (2010) 119–131.
- [81] K.L. Sheldon, E.N. Maldonado, J.J. Lemasters, T.K. Rostovtseva, S.M. Bezrukov, Phosphorylation of voltage-dependent anion channel by serine/threonine kinases governs its interaction with tubulin, *PLoS ONE* 6 (2011) e25539.
- [82] Y. Chen, M. Gaczynska, P. Osmulski, R. Polci, D.J. Riley, Phosphorylation by Nek1 regulates opening and closing of voltage dependent anion channel 1, *Biochem. Biophys. Res. Commun.* 394 (2010) 798–803.
- [83] D.J. Klionsky, H. Abeliovich, P. Agostinis, D.K. Agrawal, G. Aliev, D.S. Askew, M. Baba, E.H. Baehrecke, B.A. Bahr, A. Ballabio, B.A. Bamber, D.C. Bassham, E. Bergamini, X. Bi, M. Biard-Piechaczyk, J.S. Blum, D.E. Bredesen, J.L. Brodsky, J.H. Brumell, U.T. Brunk, W. Bursch, N. Camougrand, E. Cebollo, F. Cecconi, Y. Chen, L.S. Chin, A. Choi, C.T. Chu, J. Chung, P.G. Clarke, R.S. Clark, S.G. Clarke, C. Clave, J.L. Cleveland, P. Codogno, M.I. Colombo, A. Coto-Montes, J.M. Cregg, A.M. Cuervo, J. Debnath, F. Demarchi, P.B. Dennis, P.A. Dennis, V. Deretic, R.J. Devenish, F. Di Sano, J.F. Dice, M. Difiglia, S. Dinesh-Kumar, C.W. Distelhorst, M. Djavaheri-Mergny, F.C. Dorsey, W. Droge, M. Dron, W.A. Dunn Jr., M. Duzsenko, N.T. Eissa, Z. Elazar, A. Esclatine, E.L. Eskelinen, L. Fesus, K.D. Finley, J.M. Fuentes, J. Fuyeo, K. Fujisaki, B. Galliot, F.B. Gao, D.A. Gewirtz, S.B. Gibson, A. Gohla, A.L. Goldberg, R. Gonzalez, C. Gonzalez-Estevez, S. Gorski, R.A. Gottlieb, D. Haussinger, Y.W. He, K. Heidenreich, J.A. Hill, M. Hoyer-Hansen, X. Hu, W.P. Huang, A. Iwasaki, M. Jaattela, W.T. Jackson, X. Jiang, S. Jin, T. Johansen, J.U. Jung, M. Kadowaki, C. Kang, A. Kelekar, D.H. Kessel, J.A. Kiel, H.P. Kim, A. Kimchi, T.J. Kinsella, K. Kiselyov, K. Kitamoto, E. Knecht, M. Komatsu, E. Kominami, S. Kondo, A.L. Kovacs, G. Kroemer, C.Y. Kuan, R. Kumar, M. Kundu, J. Landry, M. Laporte, W. Le, H.Y. Lei, M.J. Lenardo, B. Levine, A. Lieberman, K.L. Lim, F.C. Lin, W. Liou, L.F. Liu, G. Lopez-Berestein, C. Lopez-Otin, B. Lu, K.F. Macleod, W. Malorni, N. Martinet, K. Matsuoka, J. Mautner, A.J. Meijer, A. Melendez, P. Michels, G. Miotto, W.P. Mistiaen, N. Mizushima, B. Mograbi, I. Monastyrska, M.N. Moore, P.I. Moreira, Y. Moriyasu, T. Motyl, C. Munz, L.O. Murphy, N.I. Naqvi, T.P. Neufeld, I. Nishino, R.A. Nixon, T. Noda, B. Nurnberg, M. Ogawa, N.L. Oleinick, L.J. Olsen, B. Ozpolat, S. Paglin, G.E. Palmer, I. Papassideri, M. Parkes, D.H. Perlmutter, G. Perry, M. Piacentini, R. Pinkas-Kramarski, M. Prescott, T. Proikas-Cezanne, N. Raben, A. Rami, F. Reggiori, B. Rohrer, D.C. Rubinsztein, K.M. Ryan, J. Sadoshima, H. Sakagami, Y. Sakai, M. Sandri, C. Sasakawa, M. Sass, C. Schneider, P.O. Seglen, O. Seleverstov, J. Settleman, J.J. Shacka, I.M. Shapiro, A. Sibirny, E.C. Silva-Zacarin, H.U. Simon, C. Simone, A. Simonsen, M.A. Smith, K. Spanel-Borowski, V. Srinivas, M. Steeves, H. Stenmark, P.E. Stromhaug, C.S. Subauste, S. Sugimoto, D. Sulzer, T. Suzuki, M.S. Swanson, I. Tabas, F. Takeshita, N.J. Talbot, Z. Talloczy, K. Tanaka, K. Tanaka, I. Tanida, G.S. Taylor, J.P. Taylor, A. Terman, G. Tettamanti, C.B. Thompson, M. Thumm, A.M. Tolkovsky, S.A. Tooz, R. Truant, L.V. Tumanovska, Y. Uchiyama, T. Ueno, N.L. Uzcategui, I. van der Klei, E.C. Vaquero, T. Vellai, M.W. Vogel, H.G. Wang, P. Webster, J.W. Wiley, Z. Xi, G. Xiao, J. Yahalom, J.M. Yang, G. Yap, X.M. Yin, T. Yoshimori, L. Yu, Z. Yue, M. Yuzaki, O. Zabirnyk, X. Zheng, X. Zhu, R.L. Deter, Guidelines for the use and interpretation of assays for monitoring autophagy in higher eukaryotes, *Autophagy* 4 (2008) 151–175.
- [84] E. Cuyas, B. Corominas-Faja, J. Joven, J.A. Menendez, Cell cycle regulation by the nutrient-sensing mammalian target of rapamycin (mTOR) pathway, *Methods Mol. Biol.* 1170 (2014) 113–144.
- [85] B. Andziak, R. Buffenstein, Disparate patterns of age-related changes in lipid peroxidation in long-lived naked mole-rats and shorter-lived mice, *Aging Cell* 5 (2006) 525–532.
- [86] M. Perluigi, G. Pupo, A. Tramutola, C. Cini, R. Coccia, E. Barone, E. Head, D.A. Butterfield, F. Di Domenico, Neuropathological role of PI3K/Akt/mTOR axis in Down syndrome brain, *Biochim. Biophys. Acta* 1842 (2014) 1144–1153.
- [87] S.W. Margulis, W. Saltzman, D.H. Abbott, Behavioral and hormonal changes in female naked mole-rats (*Heterocephalus glaber*) following removal of the breeding female from a colony, *Horm. Behav.* 29 (1995) 227–247.